Tricultured cell sheets develop into functional pancreatic islet tissue with a vascular network

Hidekazu Sekine (sekine.hidekazu@twmu.ac.jp)
Tokyo Women's Medical University https://orcid.org/0000-0001-7497-5554
Jun Homma
Tokyo Women's Medical University
Tatsuya Shimizu
Tokyo Women's Medical University

Article

Keywords:

Posted Date: August 8th, 2022

DOI: https://doi.org/10.21203/rs.3.rs-1900386/v1

Abstract

Methods to induce islet β-cells from induced pluripotent stem cells or embryonic stem cells have been established. However, islet β-cells are susceptible to apoptosis under hypoxic conditions, so the technique used to transplant β-cells must maintain the viability of the cells *in vivo*. The present study describes the development of a tricultured cell sheet, which was made by co-culturing islet β-cells, vascular endothelial cells and mesenchymal stem cells for 1 day. The islet β-cells in the tricultured cell sheet self-organized into islet-like structures surrounded by a dense vascular network *in vitro*. Triple-layered tricultured cell sheets engrafted well after transplantation *in vivo* and developed into insulin-secreting tissue with abundant blood vessels and a high density of islet β-cells. We anticipate that the tricultured cell sheet could be used as an *in vitro* pseudo-islet model for pharmaceutical testing and may have potential for development into transplantable grafts for use in regenerative medicine.

Introduction

Subcutaneous administration of exogenous insulin is an essential therapy for type 1 diabetes mellitus (DM) and an effective option for type 2 DM. The number of people with type 2 DM worldwide and global insulin requirements are predicted to rise in the near future [1]. However, insulin supplies may become unstable due to human-caused or natural disasters. Therefore, definitive therapies for DM are badly needed. Regenerative medicine offers hope as a new method of treating DM. Researchers in the field of regenerative medicine have already established methods of inducing islet β-cells from induced pluripotent stem cells (iPSCs) or embryonic stem cells (ESCs) [2], and the focus has now switched to the development of suitable techniques for transplanting islet β-cells derived from iPSCs or ESCs. The pancreas has a higher oxygen tension than the liver or kidneys [3], and the islets receive 10% of the pancreatic blood flow despite only comprising 1–2% of the pancreatic mass [4]. Since the islets have high blood flow requirements, it is essential that the method used to transplant islet β-cells maintains the viability of the cells in the graft.

Many previous studies of islet β-cells have utilized spheroids containing aggregated cells because cell-cell contact between islet β-cells has been shown to inhibit cell death and increase insulin secretion [5] and because pancreatic progenitor cells derived from iPSCs can differentiate into mature islet β-cells under aggregated conditions (in spheroids) but not under non-aggregated conditions [6]. However, an important limitation of the spheroid method is central necrosis due to hypoxia or nutrient deprivation. Islet β-cells require a stable supply of oxygen and nutrients, hence the size of an islet β-cell spheroid must be carefully regulated [5]. In addition, the transplantation of a suspension of spheroids *in vivo* results in dispersion of the transplanted cells, hence the scattered cells would be difficult to remove in the event of tumorigenesis or graft versus host disease, which are known severe adverse effects of transplantation. For the above reasons, the transplantation of spheroids is not considered an optimal method for islet β-cells derived from iPSCs or ESCs.

Previous studies have shown that cell sheets harvested from temperature-responsive culture dishes exhibit good engraftment after transplantation *in vivo* [7,8]. A cell sheet is harvested by decreasing the temperature to 20℃ without the use of protease solution. This method of harvesting a cell sheet causes minimal damage to extracellular proteins such as cell adhesion factors, cell-cell binding proteins and the extracellular matrix, which helps to maintain cell-cell interactions within the cell sheet and promotes engraftment of the cell sheet after transplantation *in vivo* [9,10]. Another advantage of cell sheets is that their thickness is constant, so the risk of central necrosis is low. Furthermore, the cells in a sheet do not disperse after transplantation because the sheet is transplanted as a contiguous two-dimensional tissue. The advantages described above potentially make cell sheets well suited to the transplantation of islet cells. Indeed, prior research demonstrated that the transplantation of cell sheets derived from islet cells attenuated hyperglycemia in a mouse model of DM [11,12]. However, mice have a small body size, hence only two layers of cell sheets were required to achieve a therapeutic effect. The application of this technique in a clinical setting would require thick tissue containing a large number of islet β-cells, but few studies have reported the construction of thick tissues comprised of islet β-cells.

Tissue composed of only one or two cell sheets is thin, hence its viability during the early phase of transplantation can be maintained by the diffusion of oxygen and essential nutrients from the surrounding tissues. Secure tissue engraftment during the later phase of transplantation is achieved by the development of a vascular network in the transplanted cell sheets. However, the central part of a large three-dimensional (3D) tissue constructed from multiple layers of cell sheets would not receive sufficient oxygen and nutrients after transplantation. As a result, the center of the tissue would undergo necrosis before a vascular network could develop. This limitation of thick graft tissue means that a vascular network must be introduced into the thick-tissue before it is transplanted. The establishment of a cell sheet-based method for constructing 3D islet β-cell tissue with a dense vascular network would facilitate the development of a transplantation technique with the potential to be applied clinically.

Previously, we reported that the transplantation of triple-layered cell sheets (i.e., three cell sheets stacked together) containing myocardial cells and vascular endothelial cells (vECs) could be used to construct 3D cardiomyocyte tissue with a vascular network *in vivo* and *in vitro* [13–16]. However, it was not known whether this method could be applied to islet β-cells, which are susceptible to apoptosis under hypoxic conditions. Therefore, an important aim of the present study was to establish whether the transplantation of a triple-layered cell sheet could be used to construct thick islet tissue with a dense vascular network. An additional objective of this study was to evaluate whether the technique could be improved by culturing islet β-cells with other cell types, namely vECs and mesenchymal stem cells (MSCs), during the creation of the cell sheets. The latter objective was achieved by comparing the results of transplantation between tricultured cell sheets (comprising islet β-cells, vECs and MSCs), cocultured cell sheets (comprising islet β-cells and MSCs), and spheroids of monocultured islet β-cells. vECs were chosen for coculture with islet β-cells because there is evidence that the viability of vECs in the pancreatic islets is more important for islet engraftment than the location of the transplant [3], which suggests that the viability of transplanted islet β-cells might be enhanced by the presence of vECs in the immediate vicinity.

MSCs were selected for the experiments because the coculture of islet β-cells with MSCs has been shown to improve insulin secretion, angiogenesis and engraftment *in vivo* [17]. Furthermore, co-transplantation with MSC sheets has been reported to enhance the engraftment and viability of pancreatic islets *in vivo* [18,19].

The findings of the present study show that tricultured cell sheets exhibited higher levels of engraftment, islet β-cell density, insulin secretion and vascularization after transplantation than cocultured cell sheets or monocultured islet β-cells.

Results

Islet β-cells assembled into small clusters under triculture conditions

Tricultured cell sheets were constructed using iGL cells (a clonal INS-1E cell line derived from rat pancreatic β-cells stably expressing a fusion protein of insulin and *Gaussia* luciferase [insulin-GLase]) [20], human adipose-derived stem cells (hASCs), and green fluorescent protein-expressing human umbilical vein endothelial cells (GFP-HUVECs). One day after cell seeding on the culture dish, the islet β-cells had assembled into small clusters among the other cells (Fig. 1a–c), and the pseudopodia of vECs were observed to infiltrate the intercellular spaces (Fig. 1d). A time-lapse video showing the clustering of islet β-cells between 1 hour and 1 day after cell seeding is shown in Supplementary Video 1. The vECs appeared to migrate and form a network between days 1 and 3 after seeding (Fig. 1d).

Culture for more than 1 day was associated with an increase in insulin secretion by islet β-cells but a decrease in cell viability

The optimal day to harvest the tricultured cells as a cell sheet was determined by evaluating the time-dependent changes in the secretion of insulin by the β-cells as well as cell viability. Insulin secretion (expressed as the luminescence intensity of insulin-GLase) in response to a 20 mM glucose load increased significantly ($P < 0.05$) between day 1 (36.1 ± 15.1 $\times 10^5$ AU) and day 2 (76.9 ± 24.7 $\times 10^5$ AU) after seeding but showed a non-significant tendency toward a decrease between day 2 and day 3 (55.6 ± 17.4 $\times 10^5$ AU; Fig. 1e). Glucose-dependent insulin secretion, expressed as the ratio of insulin-GLase luminescence in 20 mM glucose to that in 2 mM glucose, did not differ significantly between day 1 (3.6 ± 1.7), day 2 (4.6 ± 0.8) and day 3 (4.0 ± 1.7) (Fig. 1f). The cells were seeded at an over-confluent density, which is ideal for cell sheet construction. However, under these conditions, the viability of the cultured cells decreased significantly over time from 98.9% ± 0.3% on day 1 to 97.1% ± 0.3% on day 2 and 86.9% ± 5.6% on day 3 ($P < 0.05$ for all pairwise comparisons; Fig. 1d, g). Since insulin secretory function in a sheet harvested 1 day after cell seeding would likely also increase during the next 24 hours, we prioritized cell viability over insulin secretory function when selecting the optimal time for cell sheet harvesting. Therefore, in subsequent experiments, the tricultured cell sheets were harvested from the temperature-responsive culture dishes at 1 day after cell seeding.

Tricultured cells were successfully harvested from a temperature-responsive culture dish as an intact sheet at 1 day after seeding

Tricultured cells (iGL cells, GFP-HUVECs and hASCs) on a temperature-responsive culture dish could be harvested as an intact cell sheet at 1 day after seeding (Fig. 2a, b). The detached cell sheet shrank to about one-third of the diameter of the 35-mm dish (Fig. 2a), which resulted in cells overlapping in some parts of the cell sheet (Fig. 2c–e). Cocultured iGL cells and hASCs could also be harvested as a cell sheet from a temperature-responsive culture dish under the same conditions (Supplementary Fig. 1a–d). However, cell sheets could not be generated using monocultured iGL cells, likely due to the paucity of extracellular matrix (Supplementary Fig. 2a–c).

Islet β-cells and vECs in the tricultured cell sheet self-organized into pancreatic islet tissue with a dense vascular network *in vitro*

Next, changes in the morphology of the cells in the tricultured cell sheet over time were evaluated *in vitro*. The tricultured cell sheet was transplanted onto the surface of a cylindrical fibrin gel and cultured for 3 days (Fig. 3a, b). After 3 days of culture, the vECs in the tricultured cell sheet were observed to have infiltrated the intercellular spaces and connected with each other to form tubular-like structures (Fig. 3c, Supplementary Video 2). On the other hand, when the three cell types were seeded directly on the cylindrical fibrin gel (i.e., not as a cell sheet), the GFP-HUVECs did not form tubular-like structures after 3 days of culture (Supplementary Video 3). The islet β-cells in the tricultured cell sheet were observed to assemble into small clusters during the 3-day culture period (Fig. 3d). Furthermore, the clusters of islet β-cells were closely surrounded by endothelial networks and penetrated by the pseudopodia of vECs that branched off from the endothelial networks (Fig. 3d, e). These results indicate that *in vitro* culture of cell sheets containing islet β-cells, vECs and adipose-derived MSCs leads to the development of pancreatic islet tissue that is associated with a dense vascular endothelial network.

Islet β-cell sheets containing vECs exhibited the highest levels of insulin secretion after transplantation onto rat muscle *in vivo*

The insulin secretory function of monocultured islet β-cells (spheroids), cocultured cell sheets (β-cells and hASCs) and tricultured cell sheets (β-cells, hASCs and vECs) were compared after transplantation onto the gluteal muscles of athymic rats (Fig. 4a). Since it was not possible to construct cell sheets from monocultured islet β-cells (Supplementary Fig. 2a–c), monocultured islet β-cell spheroids were transplanted instead (Fig. 4b–d and Supplementary Video 4). Triple-layered cell sheets were transplanted for the triculture and coculture groups (Fig. 4e–g, Supplementary Fig. 1e, f, and Supplementary Video 5). The non-fasting blood glucose levels of the rats were not significantly different among the three groups either before transplantation or 7 days post-transplantation (Supplementary Fig. 3). However, the secretion of insulin-GLase from the engrafted iGL cells into the rat circulation at 7 days post-transplantation was significantly higher in the cocultured cell sheet group than in the monocultured spheroid group ($P < 0.01$) and significantly higher in the tricultured cell sheet group than in the cocultured cell sheet group ($P < 0.05$) or monocultured spheroid group ($P < 0.0001$) (Fig. 4h).

Transplanted islet β-cell sheets containing vECs formed a dense vascular network that connected with the vasculature of the muscle of the recipient rat

Megascopic observation of the transplantation region at 7 days post-transplantation revealed no obvious change in the surface appearance of the muscle in the monocultured spheroid group, whereas the triple-layered cell sheets were visible as a circular region on the muscle in both the tricultured cell sheet and cocultured cell sheet groups (Fig. 5a, Supplementary Fig. 4). Furthermore, the region where the tricultured cell sheets had been transplanted appeared congested with blood (Fig. 5a). Stereomicroscopy and fluorescence stereomicroscopy revealed that the region where the tricultured cell sheets had been transplanted contained a dense network of GFP-HUVECs, and this network was observed to contain blood (Fig. 5b, Supplementary Fig. 4), whereas the region where cocultured cell sheets had been transplanted appeared white and avascular (Fig. 5a, Supplementary Fig. 4). In agreement with the stereomicroscopy data, laser Doppler perfusion imaging showed that the level of blood perfusion was significantly higher for the transplanted tricultured cell sheets than for the transplanted cocultured cell sheets (710.7 ± 40.6 units vs. 508.4 ± 52.5 units, $P < 0.001$; Fig. 5c, d).

Transplanted islet β-cell sheets containing vECs engrafted successfully onto muscle and contained a high density of islet β-cells

Engraftment of the islet β-cells at 7 days after transplantation was evaluated immunohistochemically by staining the islet β-cells with an anti-insulin antibody (Fig. 6a). The engrafted area was significantly higher in the cocultured cell sheet group than in the monocultured spheroid group (0.558 ± 0.185 mm^2 vs. 0.063 ± 0.052 mm^2, $P < 0.01$) and significantly higher in the tricultured cell sheet group (0.848 ± 0.107 mm^2) than in the cocultured cell sheet group ($P < 0.05$) or monocultured spheroid group ($P < 0.001$; Fig. 6b). Representative immunofluorescence images of the region of islet β-cell engraftment are shown in Fig. 6c; the islet β-cells were immunostained for insulin (red), and the vECs were immunostained for CD31 (green). Since engraftment was much lower for the monocultured spheroids than for the other two groups, subsequent analyses of the thickness of the engrafted tissue, density of islet β-cells and density of blood vessels were carried out only for the cocultured cell sheet and tricultured cell sheet groups. The thickness of the engrafted cell sheets was numerically but non-significantly higher in the tricultured cell sheet group than in the cocultured cell sheet group (117.9 ± 28.1 μm vs. 84.2 ± 26.6 μm, $P = 0.0985$; Fig. 6d). Furthermore, the density of islet β-cells in the engrafted cell sheets was significantly higher in the tricultured cell sheet group than in the cocultured cell sheet group (33.3% ± 2.4% vs. 27.3% ± 2.7%, $P < 0.05$; Fig. 6e).

Islet β-cell sheets containing vECs developed dense vascular structures after engraftment

The vascular constructs in the engrafted cells were evaluated by immunohistochemical staining of the vECs for CD31 (Fig. 6c). Vascular structures were observed in the interstitial space between islet β-cell clusters for both engrafted cocultured cell sheets and engrafted tricultured cell sheets, whereas few vascular structures were found in the engrafted monocultured spheroids (Fig. 6c). Notably, the tricultured

cell sheet group had a significantly higher density of blood vessels than the cocultured cell sheet group (1751 ± 295 vessels/mm^2 vs. 1073 ± 137 vessels/mm^2; $P < 0.01$; Fig. 6f).

Discussion

The present research was designed to assess whether tricultured cell sheets containing islet β-cells, vECs and MSCs were capable of forming islet tissue with a dense vasculature. Our study has three major findings. First, use of the triculture method resulted in the successful construction of an islet β-cell-containing cell sheet that had a relatively tear-proof 2D structure and exhibited good viability. Second, the islet β-cells in the tricultured cell sheet self-organized into islet structures surrounded by a dense vascular network *in vitro*. Third, triple-layered tricultured sheets engrafted well after transplantation onto rat muscle and developed into insulin-secreting tissue with an abundance of blood vessels and a high density of islet β-cells.

This study successfully established a method of constructing a cell sheet containing three types of cells: islet β-cells, vECs and MSCs. Prior investigations have described other types of insulin-secreting cell sheet including a primary-culture pancreatic islet sheet and a pancreatic islet-loaded MSC sheet [11,12,18,19,21]. However, an islet β-cell sheet containing vECs has not been reported previously. Fujita et al. and Saito et al. published methods for the generation of islet cell sheets from primary rat islets or primary mouse islets, and both types of cell sheet were shown to exert a hypoglycemic effect in a mouse model of DM [11,12]. On the other hand, we were unable to construct cell sheets from iGL cells alone because the planar cell-cell connections were not maintained when the cells were detached from the temperature-responsive culture dish. The difference in results between our study and those of Fujita et al. and Saito et al. may be due to the lack of extracellular matrix (ECM)-secreting cells in our monocultured cell sheet. Nikolova et al. reported that islet β-cells do not contribute to ECM deposition in the islets [22]. Primary islets contain native MSCs and vECs that secrete ECMs, hence the presence of these cells and their deposition of ECM in the intercellular space likely permitted the generation of cell sheets from primary rat/mouse islets. Nevertheless, a support membrane was required to detach a primary islet cell sheet from a temperature-responsive culture dish and transplant it *in vivo* [11,12]. The failure of monocultured iGL cells to form a cell sheet most likely resulted from a deficiency of ECM, and this issue would arise irrespective of whether the islet β-cells were derived from iPSCs or ESCs. On the other hand, cell sheets were successfully made using a triculture method, and the tricultured cell sheet was a relatively tear-proof 2D tissue that did not require the use of a support membrane for transplantation or stacking. Furthermore, the technique used to construct tricultured cell sheets would be applicable to both iPSC- and ESC-derived islet β-cells. We anticipate that tricultured cell sheets will prove useful for tissue bioengineering.

The viability of the islet β-cells was an important factor taken into consideration during development of the method for cell sheet construction. Pancreatic islets have a higher oxygen consumption than many other tissues [23], and islet β-cells are known to undergo apoptosis under hypoxic conditions [24]. In the clinical setting, pancreatic islets must be transplanted within 2 days of harvesting from a human donor

because the viability of the islet β-cells decreases over time [25]. The construction of a cell sheet requires confluent cells, but the dissolved oxygen in the culture medium is rapidly consumed under these conditions, predisposing to progressive apoptosis of the islet β-cells. A consistent finding of our experiments was that cell viability decreased with a longer duration of culture. Based on our results, we concluded that culture for 1 day was optimal for harvesting a cell sheet from a temperature-responsive culture dish.

The component cells of the pancreatic islets are organized into clusters surrounded by mesenchymal cells in both humans and mice [26]. In addition, vECs are in close contact with and penetrate the islets. The close relationship between the islets and vECs is illustrated by the observation that only a basement membrane separates islet β-cells from vECs in some regions of the islets [27]. In the present study, islet β-cells formed small clusters at 1 day after seeding, although a vEC network was not present at this time point. However, culture of a harvested cell sheet on a fibrin gel for 3 days resulted in the assembly of islet β-cells into clusters that were separated by tubular vascular structures derived from vECs. Furthermore, some parts of the vEC network were observed to penetrate the clusters of islet β-cells. These results suggest that islet β-cells and vECs in a cell sheet self-organize into a islet structure with a dense vascular network *in vitro*. However, Supplementary Video 1 shows that formation of a vascular network did not progress well when the cells were simply seeded onto a culture dish (i.e., were not in the form of a cell sheet). Our results suggest that self-organization is promoted not only by the combination of cells but also by the structure inherent to a cell sheet. Research has shown that self-organization requires heterogeneous cell populations, ECM components and appropriate cell densities, and that differences in the interactions between the respective cell types and the ECM allow each cell type to assemble and self-organize [28,29]. Kushida et al. reported that a cell sheet undergoes 'self-shrinkage' immediately following detachment from a temperature-responsive culture dish [9]. The cell sheets in the present study shrank to about one-third of the diameter of the culture dish after their detachment, and tissue sections showed that some of the cells in the cell sheet had adopted a multi-layered structure. This shrinkage of the planar cellular tissue during detachment from the culture dish causes a rapid increase in both cell density and ECM density. We have previously described the self-organization of a cell sheet constructed using rat primary endometrial cells, which initially contained a mixture of epithelial cells and stromal cells: culturing of a re-adhered cell sheet led to the formation of a two-tiered tissue containing an epithelial layer and a stromal layer [30]. We speculate that a cell sheet may have an appropriate cell density and ECM density for self-organization as well as adhesion factors on its lower surface. Since cell sheets can be stably transferred, they could be used to construct tissues *in vitro* that would be suitable for applications such as disease modelling and drug testing. In addition, cell sheets have the potential to be stacked to create thick 3D tissues. Expanding on the present study, we believe that it will be feasible to engineer 3D pancreas-like tissue *in vitro* by combining the islet β-cell-containing tricultured cell sheet with the perfusion culture method described previously for myocardial tissue construction [14,15].

The tricultured cell sheet containing islet β-cells, vECs and MSCs did not have a vascular network on the first day of transplantation. However, the transplantation of three tricultured cell sheets (stacked to make

a triple-layered construct) onto rat subcutaneous muscle resulted in the formation of vascular-rich tissue. Notably, the tissue generated from tricultured cell sheets had a greater density of islet β-cells and higher insulin secretory function than tissue created from cocultured cell sheets that lacked vECs. Moreover, the tissue that developed from tricultured cell sheets was thicker and had a higher density of islet β-cells than tissue obtained by transplanting islet β-cell sheets onto the liver [12,19], despite the fact that our sheet was transplanted onto a less vascular region. There is evidence that MSCs can improve islet engraftment and insulin secretion by exerting angiogenic, immunosuppressive and antiapoptotic effects through the secretion of trophic factors such as vascular endothelial growth factor, hepatocyte growth factor, interleukin-6 and transforming growth factor-β [17,31]. Hirabaru et al. and Lee et al. reported that pancreatic islet-loaded MSC sheets exhibited good engraftment and angiogenesis after transplantation and were capable of attenuating hyperglycemia in a mouse model of DM [18,19]. Our results consistently showed that cocultured cell sheets containing islet β-cells and MSCs exhibited substantially better engraftment and insulin secretion after transplantation than monocultured islet β-cell spheroids. Moreover, tricultured cell sheets demonstrated a larger region of engraftment, a greater abundance of blood vessels and a higher level of insulin secretion after transplantation than cocultured cell sheets.

However, since the cell sheets in the present study were transplanted before they had formed a vascular network, they were dependent on the diffusion of oxygen and nutrients from the surrounding tissues during the early phase of transplantation. Thus, differences in viability between tricultured cell sheets and cocultured cell sheets cannot be explained solely by differences in blood vessel formation within the cell sheet. It has been reported that vECs and islet β-cells interact with each other via paracrine factors and that ECM secreted by vECs exerts an anti-apoptotic effect on islet β-cells and increases their bioactivity. The vEC-islet interaction is thought to be efficient *in vivo* because the cells are in close contact with each other [4,27,32]. In the present study, the transplanted islet β-cells and vECs were in close contact with each other within the cell sheet, and this may have enhanced the viability of the tricultured cell sheet due to anti-apoptotic effects exerted via the vEC-islet axis. On the other hand, long-term engraftment of islet β-cells requires a stable supply of oxygen and nutrients through a vascular network. The present study demonstrates that transplanted vECs are able to establish a vascular network that communicates with the recipient's blood vessels within 1 week. This result suggests that an islet β-cell sheet containing vECs has the potential to self-organize into pseudo-islets with an abundant vascular network that would show stable engraftment in the long term. We suggest that the tricultured cell sheet described in this study is well suited to transplantation *in vivo* because the presence of vECs in the immediate vicinity of the islet β-cells supports early and late engraftment of the islet β-cell tissue through vEC-β-cell interactions and the formation of a vascular network.

We anticipate that further advances in regenerative medicine techniques will allow islet β-cells derived from iPSCs and ESCs to be applied in the clinical setting, although two important challenges will need to be overcome for this to happen. First, stem cell-derived β-cells are not sufficiently mature to exert a hypoglycemic effect, so methods will need to be developed to promote tissue maturation *in vivo.* Second, it will be necessary to establish an approach to removing engrafted cells in the event of serious adverse

effects such as tumor formation or graft-versus host disease. Toyoda et al. found that cell-cell contacts between islet β-cells in a spheroid promoted the differentiation and maturation of islet β-cells derived from iPSCs [6]. Moreover, coculture with vECs was reported to promote the differentiation of ESC-derived and iPSC-derived pancreatic progenitor cells into mature pancreatic islet beta cells [33,34]. Our tricultured sheet contains vECs and thus meets the above conditions for the maturation of stem cell-derived β-cells. Additionally, the present study showed that the transplantation of tricultured cell sheets resulted in the engraftment of viable islet β-cells and the development of an abundant vascular network. Therefore, a thick insulin-secreting tissue potentially could be constructed in the subcutaneous space by stacking tricultured cell sheets in a multistep method, as previously used to engineer thick cardiac tissue [13,14,16,35]. Sequential stacking of triple-layered tricultured cell sheets may have the potential to generate a single mass of mature islet β-cell tissue that could be removed in the event of a severe adverse effect. Thus, we believe that our novel procedure is an attractive option for development into a technique for transplanting stem cell-derived islet β-cells.

Conclusion

Tricultured cell sheets constructed from islet β-cells, MSCs and vECs may have an ECM-rich environment that promotes self-organization into islet tissue with an abundant vascular network *in vitro* and *in vivo*. The tricultured cell sheet described in this study could be used as a pseudo-islet model for pharmaceutical testing *in vitro* and may have potential for development into a transplantable graft for use *in vivo* as a regenerative therapy.

Materials And Methods

Ethics

All animal experiments were approved by the Ethics Committee for Animal Experimentation of Tokyo Women's Medical University and performed according to the Guidelines of Tokyo Women's Medical University on Animal Use. All animals were housed in individual cages with free access to food and water and maintained at constant room temperature and humidity under a 12-hour light cycle.

Culture of cells

The rat pancreatic β-cell line, iGL, was provided by Cosmo Bio (Tokyo, Japan) and used at passage 4–9. The cells were cultured in IGLM medium (Cosmo Bio). ASCs were provided by Lonza Japan (Tokyo, Japan) and used at passage 3–9. The cells were cultured in KBM-1 medium (Kohjin Bio, Saitama, Japan) containing 1% penicillin-streptomycin (Life Technologies, Rockville, MD, USA). GFP-HUVECs were provided by Angio-Proteome (Boston, MA, USA) and used at passage 3–9. The cells were cultured in VEC-1 medium (Kohjin Bio).

Preparation of the medium used for the construction of cell sheet and spheroids

To reduce the risk of vEC dysfunction due to the high glucose level in the medium [36], the concentration of D-glucose in the medium was adjusted to 8.8 mM by mixing DMEM/F12 medium containing 17.5 mM D-glucose (Thermo Fisher Scientific, Waltham, MA, USA) with D-glucose-free DMEM/F12 medium (Nacalai Tesuque, Kyoto, Japan) in a 1:1 ratio. For the construction of cell sheets and spheroids, the medium was adjusted by the addition of 10% fetal bovine serum (FBS), 1% penicillin-streptomycin and 0.007 mM L-ascorbic acid (Fujifilm Wako Pure Chemical, Osaka, Japan). Additionally, 0.5 μg laminin-332 (Reprocell, Kanagawa, Japan) was added to each well immediately after the cells had been seeded.

Preparation of cocultured and tricultured cell sheets

The tricultured cell sheets were made from iGL cells, GFP-HUVECs and hASCs in a ratio of 9:2:6. The cocultured cell sheets were constructed from iGL cells and hASCs in a ratio of 9:8. Both types of cell sheet were developed using a 35-mm temperature-responsive dish (Up cell E-type: CellSeed, Tokyo, Japan). The dish was coated with FBS overnight, and then 1.6×10^6 cells were seeded onto the dish and cultured at 37°C in a humidified atmosphere containing 5% CO_2. The next day, the cells were transferred to another incubator for 1 hour at 20°C to detach them as an intact cell sheet (Fig. 2a–c, Supplementary Fig. 1a–d). Three cell sheets were stacked as a triple-layered construct for transplantation into rats (Fig. 4e, f and Supplementary Fig. 1a, f).

Construction of monocultured islet β-cell sheets

A silicone frame was attached to the surface of a 35-mm temperature-responsive dish (Up cell E-type: CellSeed) to restrict the cell culture area to a 10-mm-diameter circular region. The cell culture area for construction of islet β-cell sheets has been described in a previous paper [12]. The cell culture area was coated with FBS overnight. Then, 9×10^5 iGL cells were seeded onto the cell culture area and cultured at 37°C in a humidified atmosphere containing 5% CO_2. The silicone frame was removed the next day, and the cells were transferred to another incubator for 1 hour at 20°C (Supplementary Fig. 2a–c).

Preparation of islet β-cell spheroids

β-cell spheroids were generated by seeding 9×10^5 iGL cells onto a 35-mm EZSPHERE plate (microwell type #900; microwell size: diameter 400–500 μm, depth 100–200 μm; AGC Techno Glass, Shizuoka, Japan) and culturing the cells at 37°C in a humidified atmosphere containing 5% CO_2. A total of three plates were used to ensure that the total number of iGL cells (27×10^5 iGL cells) was equal to that of a three-layered tricultured/cocultured cell sheet. The next day, the iGL cells had aggregated to form a spheroid in the microwell (Fig. 4b). All spheroids were collected and suspended in 90 μL saline (Fig. 4c). The transplantation procedure was performed using a 1-mL syringe with a 27G needle.

Evaluation of the viability of tricultured cells seeded on a culture dish

iGL cells, GFP-HUVECs and hASCs (same ratio and number as for tricultured cell sheets) were seeded on a 35-mm culture dish. The cells were stained with propidium iodide (PI; Thermo Fisher Scientific) and

Hoechst 33342 (NuncBlue Live cell Stain ReadyProbes reagent; Thermo Fisher Scientific) on days 1, 2 and 3 after cell seeding. PI was used as a marker of dead cells. Then, three random fields per well were captured by a fluorescence microscope at a magnification of ×100 (ECLIPSE Ts2 FL, Nikon, Tokyo, Japan). In each fluorescence image, the numbers of Hoechst-positive cells and PI-positive cells were counted using ImageJ 1.53n (National Institutes of Health, Bethesda, MA, USA), and the ratio of the number of PI-positive cells to the number of Hoechst-positive cells was calculated as a measure of viability. The average of the values for the three fields was taken as the value for the well.

Measurement of the luminescence of insulin-GLase secreted from iGL cells *in vitro*

iGL cells, GFP-HUVECs and hASCs (same ratio and number as for tricultured cell sheets) were seeded on a 35-mm culture dish. The luminescence activity of insulin-GLase was measured on days 1, 2 and 3 after cell seeding, as follows. The cells were washed in Hank's balanced salt solution (Nacalai Tesque) and pre-incubated for 1 hour in HEPES-balanced Krebs-Ringer bicarbonate buffer containing 0.01% bovine serum albumin (BSA-KRH) and 2 mM glucose (Cosmo Bio). Next, the cells were incubated for 30 minutes in 1 mL 0.01% BSA-KRH containing 2 mM glucose and then for 30 minutes in 1 mL 0.01% BSA-KRH containing 20 mM glucose. The medium in the well was collected after each 30-minute incubation and centrifuged at ×800*g* for 5 minutes. The supernatant (10 μL) was used for measurement of the GLase luminescence activity following the addition of 100 μL of the coelenterazine (CTZ)-containing buffer provided in the luciferase assay kit (Cosmo Bio). The maximal light intensity was measured at 1000 ms using a Nivo multimode plate reader (Perkin Elmer, Waltham, MA, USA). The mean value of three independent measurements was used for each experimental condition.

Imaging of islet β-cells and vECs before and after detachment of the cell sheet

The morphological characteristics of the islet β-cells and GFP-expressing vECs before and after detachment of the tricultured cell sheet were evaluated by staining iGL cells with Cell Explorer Live Cell Tracking Kit Orange Fluorescence (AAT Bioquest, Sunnyvale, CA, USA) before the cells were seeded onto a 35-mm temperature-responsive dish. The cells were imaged using a confocal microscopy system (FV1200 and FV10-ASW; Olympus, Tokyo, Japan).

Time-lapse live-cell imaging of islet β-cells and vECs during the first 22 hours after cell seeding

To monitor dynamic changes in vEC morphology under confluent conditions, the three cell types were imaged from 1 hour to 22 hours after seeding using a time-lapse live-cell imaging system (LCV110, Olympus). Islet β-cells (iGL cells) were stained with Cell Explorer Live Cell Tracking Kit Orange Fluorescence as described above. The three types of cells were seeded on a 35-mm glass-bottom dish (Matsunami Glass, Osaka, Japan) coated with FBS and cultured in 2 mL DMEM/F12 medium containing 10% FBS and 1% penicillin-streptomycin. The well was inserted into the incubator of a time-lapse live-cell imaging system (37°C, 5% CO_2). 'Orange' and 'green' (GFP) fluorescence images were captured every hour for 22 hours.

Time-lapse live-cell imaging of vECs in a tricultured cell sheet

Dynamic alterations in vEC morphology were compared between freshly harvested cell sheets and confluent cells that had been seeded 24 hours previously. Images were captured with a time-lapse live-cell imaging system (LCV110, Olympus). Fibrin gel (400 μL) [37] was applied to a 35-mm glass-bottom dish (Matsunami Glass). For the comparative analysis, one dish was seeded with the three cell types (same ratio and number as for the tricultured cell sheet) and incubated at 37°C for 24 hours, and another dish was transplanted with a freshly harvested single tricultured cell sheet (which had been incubated for 24 hours during its construction). Then, 2 mL of DMEM/F12 medium containing 10% FBS and 1% penicillin-streptomycin was gently poured into each dish, which was inserted into the incubator of a time-lapse live-cell imaging system (37°C, 5% CO_2). GFP images were captured every hour for 48 hours.

Transplantation of a tricultured cell sheet onto a cylindrical fibrin gel

To maintain the viability of the β-cells *in vitro*, a cylindrical fibrin gel with a diameter of 12 mm was set on a 35-mm dish. The cylindrical fibrin gel was constructed by pouring fibrin gel into a cylindrical silicone frame and then removing the silicone frame after 30 minutes. A single tricultured cell sheet was transplanted onto the fibrin gel, and 3 mL of DMEM/F12 medium containing 10% FBS and 1% penicillin-streptomycin was gently poured around and over the cell sheet. The cell sheet was cultured in an incubator at 37°C in 5% CO_2 (Fig. 3a, b).

Transplantation of cell sheets and spheroids into athymic rats

Male Fischer 344 athymic rats (F344/NJcl-*rnu/rnu*; 280–400 g; CLEA Japan, Tokyo, Japan) were used as the recipients. Fourteen rats were divided into three groups (Fig. 4a): a monocultured spheroid group (n = 4) for transplantation of iGL cell spheroids (Fig. 4b, c); a cocultured cell sheet group (n = 5) for transplantation of a triple-layered cocultured cell sheet construct (Supplementary Fig. 1e, f), and a tricultured cell sheet group (n = 5) for transplantation of a triple-layered tricultured cell sheet construct (Fig. 4e, f). Blood was taken from the tail vein of each rat before and 7 days after transplantation for measurement of non-fasting blood glucose levels (Glutest Neo Super; Sanwa Chemistry Laboratory, Nagoya, Japan). The rats of all groups were transplanted with the same number of iGL cells (27×10^5 cells). For the transplantation procedure, the rat was anesthetized with 2–4% inhaled isoflurane, and an incision was made on the left side of the dorsal skin to expose the superficial gluteal muscles. Then, a triple-layered cell sheet construct (tricultured or cocultured cell sheet group) was transplanted onto the muscle using a piece of polyethylene sheet (Fig. 4g, Supplementary Video 5) or spheroids (monocultured spheroid group) were injected into the superficial layer of the muscle (Fig. 4d, Supplementary Video 4). The transplanted cell sheet was covered with a porous ethylene-vinyl alcohol membrane (EVAL^{TM} membrane; Kuraray Co., Ltd., Tokyo Japan) to inhibit its adhesion to surrounding tissue. In the spheroid group, the region of transplantation was marked with sutures after the injection. Finally, the skin was sutured. Blood perfusion imaging was performed in an additional four rats, in which both a triple-layered

tricultured cell sheet and a triple-layered cocultured cell sheet were transplanted onto the superficial gluteal muscles on different sides of the body.

Imaging devices

Images of the cell sheets (Fig. 2a, Fig. 3b, Fig. 4e, Fig. 5a, Supplementary Fig. 1e, and Supplementary Fig. 2a) were captured by a camera (IXY 650, Cannon, Tokyo, Japan). The images and videos of the procedures used in the animal experiments (Fig. 4d, g, Supplementary Video 4, and Supplementary Video 5) were obtained using a stereomicroscope with an image capturing system (M651, Leica Microsystems, Wetzlar, Germany; 3CCD camera, Toshiba Corp., Tokyo, Japan; and Video Capture Box, I-O Data Device, Kanazawa, Japan). Images of cells before and after transplantation (Fig. 2b, Fig. 4c, f, Fig. 5b, and Supplementary Fig. 4) were captured using a fluorescence stereomicroscopy system (MVX10 and cellSens Dimension, Olympus).

Laser Doppler imaging of blood perfusion in the transplanted cell sheets

Relative values of blood perfusion in the transplanted cell sheets were measured using a laser Doppler perfusion imaging system (MoorLDI2-IR; Moor Instruments, Devon, UK). The perfusion signal of each image was subdivided into 16 color shades, with low-to-no perfusion displayed as dark blue and the highest level of perfusion displayed as red. The average perfusion value for each cell sheet region was calculated based on the colored histogram pixels.

Resection of engrafted islet β-cell tissue for histological analyses

Each rat was anesthetized with 2% inhaled isoflurane at 7 days after cell transplantation. First, a blood sample was obtained by cardiopuncture via the transthoracic approach. Then, the transplanted tissue was exposed and excised along with the superficial gluteal muscle. The tissue was fixed in 4% paraformaldehyde and routinely processed into 7 μm-thick paraffin-embedded sections. The sections were stained with hematoxylin-eosin and immunostained for insulin and CD31.

Measurement of the luminescence of insulin-GLase in rat serum

Immediately after its collection from the rat, the blood sample was centrifuged at ×800*g* for 15 min to obtain blood serum, and the serum was stored at -80°C to allow all serum samples to be analyzed at the same time. At the time of the analysis, all cryopreserved blood serum samples were thawed on ice in the dark. The luminescence activity of GLase in each serum sample (20 μL) was measured by the addition of 100 μL of the CTZ-containing buffer provided in the luciferase assay kit (Cosmo Bio). The maximal light intensity was measured over 5 seconds using a Nivo multimode plate reader (Perkin Elmer). The serum sample from each rat was assayed three times, and the mean value of the three measurements was used for the analysis.

Immunofluorescence staining

Sections of transplanted tissue and cell sheets were subjected to immunofluorescence staining as described in a previous report [38]. Deparaffinized sections were incubated first with anti-insulin and anti-CD31 primary antibody for 2 hours at room temperature and then with appropriate secondary antibody and nuclear staining solution for 40 minutes at room temperature (Table 1). A fluorescence microscopy system (BZ-9000; Keyence, Osaka, Japan) was used to capture images of the entire region of islet β-cell engraftment, and confocal microscopy (FV1200 and FV10-ASW) was used to capture magnified images of the region.

Table 1. Reagents used for immunohistochemistry.

Name	Catalog no.	Dilution	Source
Primary antibodies			
Guinea pig anti-insulin polyclonal antibody	ab7842	1:100	Abcam, Cambridge, UK
Rabbit anti-CD31 polyclonal antibody	RB-10333	1:10	Thermo Fisher Scientific, Waltham, MA, USA
Secondary antibodies			
Alexa Fluor 594-conjugated anti-guinea pig IgG	A11076	1:200	Life Technologies, Carlsbad, CA, USA
Alexa Fluor 488-conjugated anti-rabbit IgG	A11008	1:200	Life Technologies, Carlsbad, CA, USA
Other			
Hoechst 33258	94403	1:300	Merck, Darmstadt, Germany

Abbreviations: CD, cluster of differentiation; IgG, immunoglobulin G.

Evaluation of the immunofluorescence images of cell sheets after engraftment

Images of the entire region of islet β-cell engraftment were used to calculate the engrafted area and engrafted cell sheet thickness. The thickness of the cell sheet in each field was calculated by dividing the area of the region surrounded by insulin-positive cells by the length of the region. The average value obtained from three different sections of each sheet was used for the analysis. Then, magnified images were used to calculate the islet β-cell density and number of vessels in the engrafted cell sheets. The islet β-cell density in each field was calculated as: (insulin-positive cell area / area of the region surrounded by insulin-positive cells)×100 (%). The number of blood vessels in the region surrounded by insulin-positive cells was counted and expressed in terms of number of vessels/mm^2. The area and length measurements were obtained using ImageJ 1.53n. The average of the values for three magnified fields

was taken as the value for the section, and the average value obtained from three different sections of each cell sheet was used for the analysis.

Statistical analysis

All values are shown as the mean ± standard deviation of the mean (SDM). Two groups were compared using the paired Student's t-test, and multiple groups were compared using Tukey's honestly significant difference post-test. $P < 0.05$ was considered significant.

Declarations

Acknowledgments

This research was supported by JSPS KAKENHI grants (no. 21K12654 and 22H03944). We thank OxMedComms (www.oxmedcomms.com) for writing assistance.

Competing interests

Tokyo Women's Medical University received research funding from CellSeed Inc. and Kuraray Co., Ltd. Tatsuya Shimizu is a shareholder of CellSeed Inc. The other authors have no financial conflicts or competing interests to disclose.

Author contributions

J.H., H.S. and T.S. were involved in the design of the experiments. J.H. conducted the experiments. J.H. and H.S. analyzed the data. J.H., H.S. and T.S. wrote the paper. J.H., H.S. and T.S. initiated the project. All authors discussed the results, commented on the paper and approved the final version.

Data availability

The data that support the findings of this study are available from the corresponding

author upon reasonable request.

References

1. Basu, S. *et al.* Estimation of global insulin use for type 2 diabetes, 2018–30: a microsimulation analysis. *The Lancet Diabetes & Endocrinology* **7**, 25-33, doi:10.1016/s2213-8587(18)30303-6 (2019).
2. Pellegrini, S., Piemonti, L. & Sordi, V. Pluripotent stem cell replacement approaches to treat type 1 diabetes. *Curr Opin Pharmacol* **43**, 20-26, doi:10.1016/j.coph.2018.07.007 (2018).
3. Carlsson, P. O., Palm, F., Andersson, A. & Liss, P. Markedly decreased oxygen tension in transplanted rat pancreatic islets irrespective of the implantation site. *Diabetes* **50**, 489-495,

doi:10.2337/diabetes.50.3.489 (2001).

4. Narayanan, S. *et al.* Intra-islet endothelial cell and β-cell crosstalk: Implication for islet cell transplantation. *World journal of transplantation* **7**, 117-128, doi:10.5500/wjt.v7.i2.117 (2017).
5. Bernard, A. B., Lin, C. C. & Anseth, K. S. A microwell cell culture platform for the aggregation of pancreatic β-cells. *Tissue Eng Part C Methods* **18**, 583-592, doi:10.1089/ten.TEC.2011.0504 (2012).
6. Toyoda, T. *et al.* Cell aggregation optimizes the differentiation of human ESCs and iPSCs into pancreatic bud-like progenitor cells. *Stem Cell Res* **14**, 185-197, doi:10.1016/j.scr.2015.01.007 (2015).
7. Homma, J., Sekine, H., Matsuura, K., Kobayashi, E. & Shimizu, T. Mesenchymal Stem Cell Sheets Exert Antistenotic Effects in a Rat Arterial Injury Model. *Tissue Eng Part A* **24**, 1545-1553, doi:10.1089/ten.TEA.2018.0030 (2018).
8. Sekine, H. *et al.* Cardiac cell sheet transplantation improves damaged heart function via superior cell survival in comparison with dissociated cell injection. *Tissue Eng Part A* **17**, 2973-2980, doi:10.1089/ten.tea.2010.0659 (2011).
9. Kushida, A. *et al.* Decrease in culture temperature releases monolayer endothelial cell sheets together with deposited fibronectin matrix from temperature-responsive culture surfaces. *J Biomed Mater Res* **45**, 355-362 (1999).
10. Okano, T., Yamada, N., Sakai, H. & Sakurai, Y. A novel recovery system for cultured cells using plasma-treated polystyrene dishes grafted with poly(N-isopropylacrylamide). *J Biomed Mater Res* **27**, 1243-1251, doi:10.1002/jbm.820271005 (1993).
11. Saito, T. *et al.* Reversal of diabetes by the creation of neo-islet tissues into a subcutaneous site using islet cell sheets. *Transplantation* **92**, 1231-1236, doi:10.1097/TP.0b013e3182375835 (2011).
12. Fujita, I., Utoh, R., Yamamoto, M., Okano, T. & Yamato, M. The liver surface as a favorable site for islet cell sheet transplantation in type 1 diabetes model mice. *Regen Ther* **8**, 65-72, doi:10.1016/j.reth.2018.04.002 (2018).
13. Shimizu, T. *et al.* Polysurgery of cell sheet grafts overcomes diffusion limits to produce thick, vascularized myocardial tissues. *FASEB journal : official publication of the Federation of American Societies for Experimental Biology* **20**, 708-710, doi:10.1096/fj.05-4715fje (2006).
14. Sekine, H. *et al.* In vitro fabrication of functional three-dimensional tissues with perfusable blood vessels. *Nat Commun* **4**, 1399, doi:10.1038/ncomms2406 (2013).
15. Sakaguchi, K. *et al.* In vitro engineering of vascularized tissue surrogates. *Sci Rep* **3**, 1316, doi:10.1038/srep01316 (2013).
16. Endo, Y. *et al.* Bioartificial pulsatile cuffs fabricated from human induced pluripotent stem cell-derived cardiomyocytes using a pre-vascularization technique. *NPJ Regen Med* **7**, 22, doi:10.1038/s41536-022-00218-7 (2022).
17. Akolpoglu, M. B. *et al.* Recent advances in the design of implantable insulin secreting heterocellular islet organoids. *Biomaterials* **269**, 120627, doi:10.1016/j.biomaterials.2020.120627 (2021).

18. Hirabaru, M. *et al.* A Method for Performing Islet Transplantation Using Tissue-Engineered Sheets of Islets and Mesenchymal Stem Cells. *Tissue Eng Part C Methods* **21**, 1205-1215, doi:10.1089/ten.TEC.2015.0035 (2015).
19. Lee, Y. N. *et al.* Evaluation of Multi-Layered Pancreatic Islets and Adipose-Derived Stem Cell Sheets Transplanted on Various Sites for Diabetes Treatment. *Cells* **9**, doi:10.3390/cells9091999 (2020).
20. Suzuki, T., Kanamori, T. & Inouye, S. Quantitative visualization of synchronized insulin secretion from 3D-cultured cells. *Biochem Biophys Res Commun* **486**, 886-892, doi:10.1016/j.bbrc.2017.03.105 (2017).
21. Imamura, H. *et al.* An engineered cell sheet composed of human islets and human fibroblast, bone marrow-derived mesenchymal stem cells, or adipose-derived mesenchymal stem cells: An in vitro comparison study. *Islets* **10**, e1445948, doi:10.1080/19382014.2018.1445948 (2018).
22. Nikolova, G. *et al.* The vascular basement membrane: a niche for insulin gene expression and Beta cell proliferation. *Dev Cell* **10**, 397-405, doi:10.1016/j.devcel.2006.01.015 (2006).
23. Buchwald, P. FEM-based oxygen consumption and cell viability models for avascular pancreatic islets. *Theor Biol Med Model* **6**, 5, doi:10.1186/1742-4682-6-5 (2009).
24. Moritz, W. *et al.* Apoptosis in hypoxic human pancreatic islets correlates with HIF-1alpha expression. *FASEB journal : official publication of the Federation of American Societies for Experimental Biology* **16**, 745-747, doi:10.1096/fj.01-0403fje (2002).
25. Murdoch, T. B., McGhee-Wilson, D., Shapiro, A. M. J. & Lakey, J. R. T. Methods of Human Islet Culture for Transplantation. *Cell Transplant* **13**, 605-618, doi:10.3727/000000004783983602 (2004).
26. Dolensek, J., Rupnik, M. S. & Stozer, A. Structural similarities and differences between the human and the mouse pancreas. *Islets* **7**, e1024405, doi:10.1080/19382014.2015.1024405 (2015).
27. Peiris, H., Bonder, C. S., Coates, P. T., Keating, D. J. & Jessup, C. F. The beta-cell/EC axis: how do islet cells talk to each other? *Diabetes* **63**, 3-11, doi:10.2337/db13-0617 (2014).
28. Cerchiari, A. E. *et al.* A strategy for tissue self-organization that is robust to cellular heterogeneity and plasticity. *Proc Natl Acad Sci U S A* **112**, 2287-2292, doi:10.1073/pnas.1410776112 (2015).
29. Laurent, J. *et al.* Convergence of microengineering and cellular self-organization towards functional tissue manufacturing. *Nat Biomed Eng* **1**, 939-956, doi:10.1038/s41551-017-0166-x (2017).
30. Takagi, S. *et al.* Reconstruction of functional endometrium-like tissue in vitro and in vivo using cell sheet engineering. *Biochem Biophys Res Commun* **446**, 335-340, doi:10.1016/j.bbrc.2014.02.107 (2014).
31. Ohmura, Y. *et al.* Combined transplantation of pancreatic islets and adipose tissue-derived stem cells enhances the survival and insulin function of islet grafts in diabetic mice. *Transplantation* **90**, 1366-1373, doi:10.1097/TP.0b013e3181ffba31 (2010).
32. Nyqvist, D. *et al.* Donor Islet Endothelial Cells in Pancreatic Islet Revascularization. *Diabetes* **60**, 2571-2577, doi:10.2337/db10-1711 (2011).

33. Jaramillo, M., Mathew, S., Mamiya, H., Goh, S. K. & Banerjee, I. Endothelial cells mediate islet-specific maturation of human embryonic stem cell-derived pancreatic progenitor cells. *Tissue Eng Part A* **21**, 14-25, doi:10.1089/ten.TEA.2014.0013 (2015).
34. Talavera-Adame, D. *et al.* Effective endothelial cell and human pluripotent stem cell interactions generate functional insulin-producing beta cells. *Diabetologia* **59**, 2378-2386, doi:10.1007/s00125-016-4078-1 (2016).
35. Komae, H. *et al.* Three-dimensional functional human myocardial tissues fabricated from induced pluripotent stem cells. *Journal of Tissue Engineering and Regenerative Medicine* **11**, 926-935, doi:10.1002/term.1995 (2017).
36. Sheetz, M. J. & King, G. L. Molecular understanding of hyperglycemia's adverse effects for diabetic complications. *Jama* **288**, 2579-2588, doi:10.1001/jama.288.20.2579 (2002).
37. Tobe, Y. *et al.* Perfusable vascular tree like construction in 3D cell-dense tissues using artificial vascular bed. *Microvasc Res*, 104321, doi:10.1016/j.mvr.2022.104321 (2022).
38. Homma, J., Shimizu, S., Sekine, H., Matsuura, K. & Shimizu, T. A novel method to align cells in a cardiac tissue-like construct fabricated by cell sheet-based tissue engineering. *J Tissue Eng Regen Med* **14**, 944-954, doi:10.1002/term.3074 (2020).

Figures

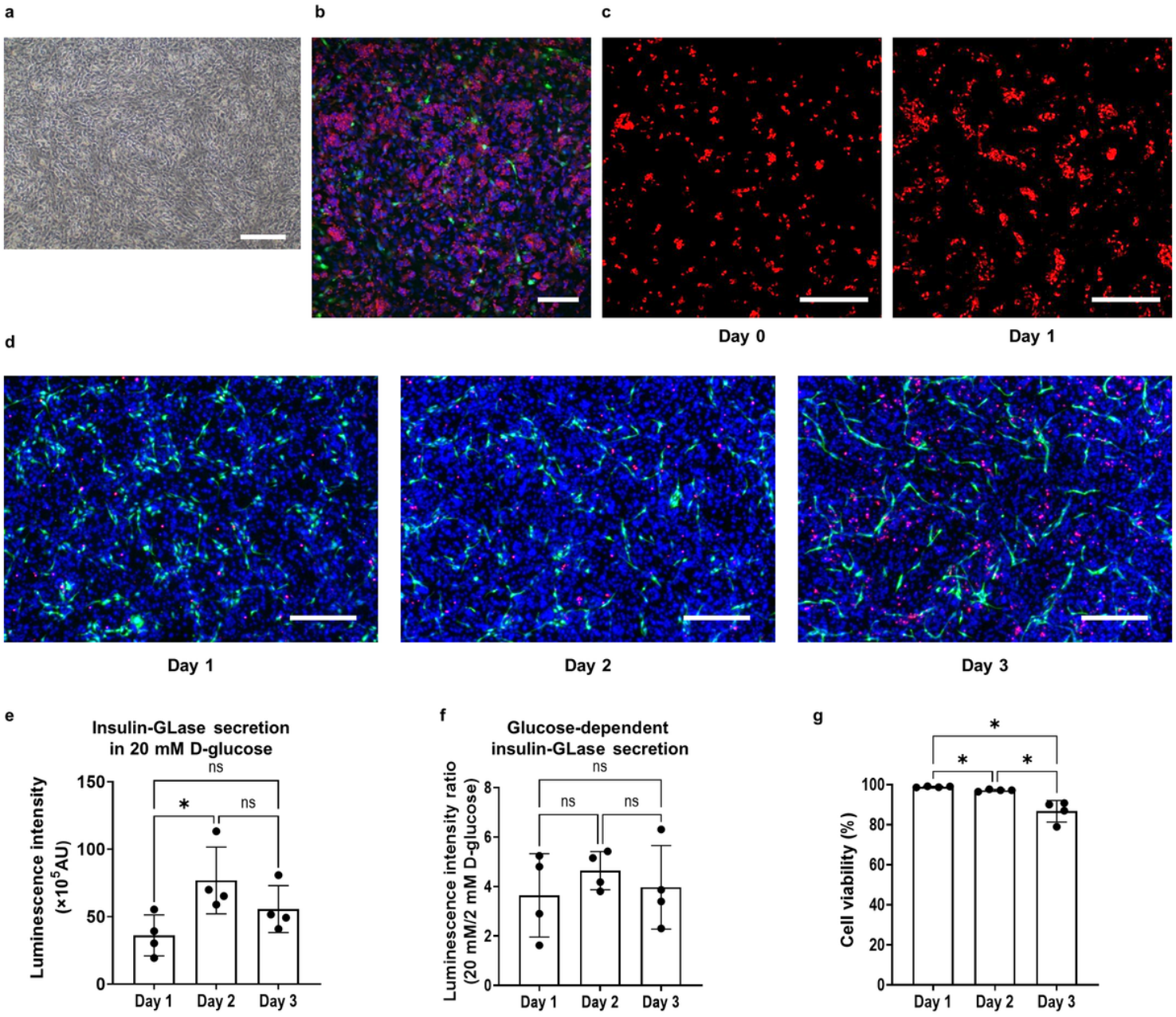

Figure 1

Morphology, viability and function of cells in the tricultured cell sheet

(a) Representative phase-contrast microscopy image of iGL cells, GFP-HUVECs and hASCs 1 day after seeding. Scale bar: 500 μm. (b) Confocal fluorescence microscopy image obtained 1 day after seeding showing GFP-HUVECs (green) and islet β-cells stained with a live-cell tracking kit (red). Nuclei are stained blue. Scale bar: 200 μm. (c) Confocal fluorescence microscopy images showing islet β-cells (stained red with a live-cell tracking kit) at 1 hour and 1 day after seeding. Scale bar: 200 μm. (d) Series of fluorescence microscopy images obtained on successive days showing the morphology of GFP-HUVECs (green) as well as dead cells (stained red with propidium iodide). Nuclei are stained blue (Hoechst

33342). Scale bar: 500 μm. (e) Insulin secretion by iGL cells evaluated through measurement of insulin-GLase luminescence intensity in 20 mM glucose-containing medium. The values are shown as the mean ± SDM (n = 4 per group). * P < 0.05; ns, not significant. (f) Glucose-dependent insulin secretion by iGL cells evaluated as the ratio of insulin-GLase luminescence intensity in 20 mM glucose-containing medium to that in 2 mM glucose-containing medium. The values are shown as the mean ± SDM (n = 4 per group). ns, not significant. (g) Cell viability under triculture conditions. The values are shown as the mean ± SDM (n = 4 per group). * P < 0.05.

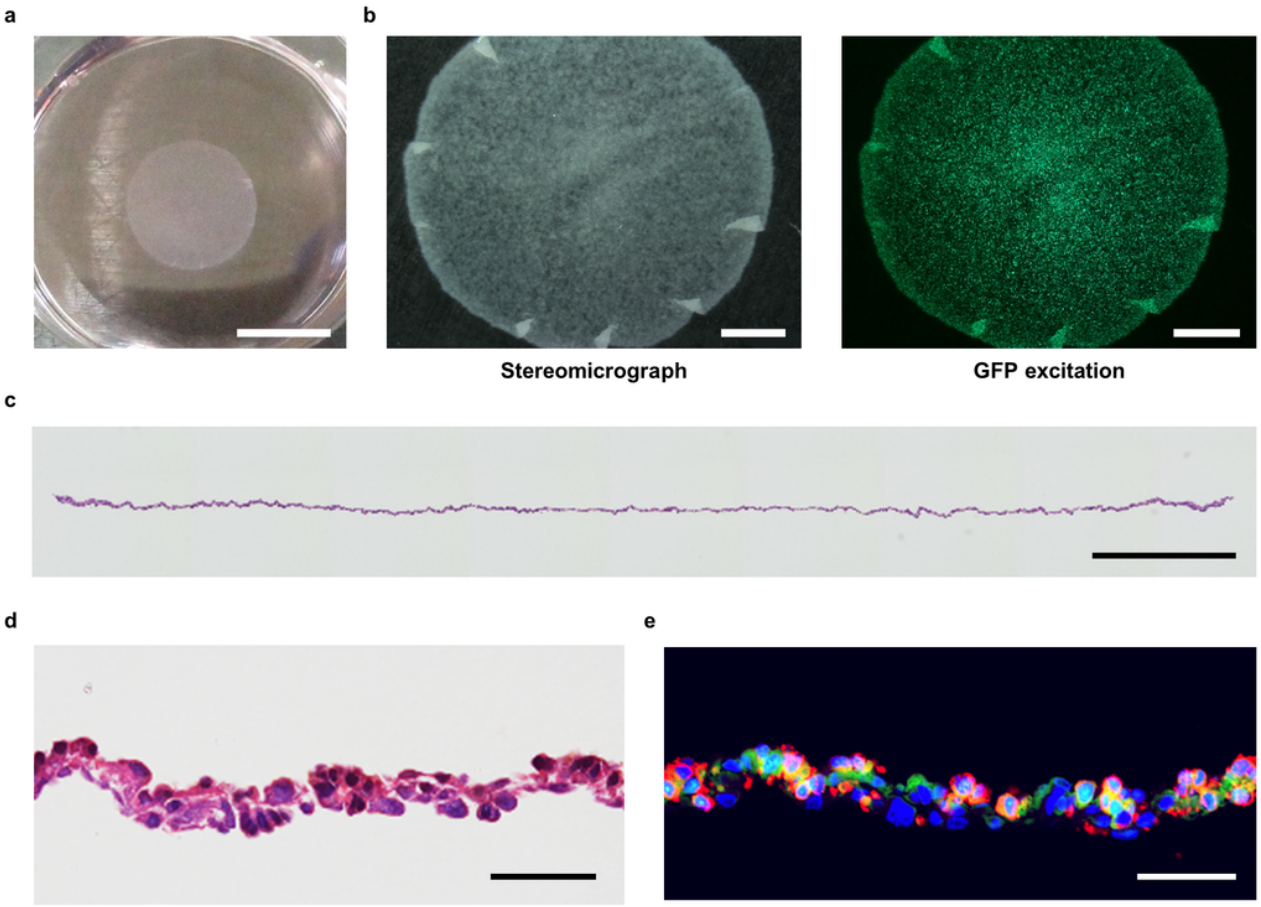

Figure 2

Morphology of the tricultured cell sheet

(a) Representative image of a tricultured cell sheet captured from directly above with a regular camera. Scale bar: 10 mm. (b) Representative images of a tricultured cell sheet captured with a stereomicroscope (left) and a fluorescence stereomicroscope (right). Green indicates GFP-HUVECs. Scale bar: 2 mm. (c) Representative cross-sectional image of a tricultured cell sheet captured with a microscope. The tricultured cell sheet was stained with hematoxylin and eosin. Scale bar: 1 mm. (d) Magnified image of

(c). Scale bar: 50 μm. (e) Representative cross-sectional image of a tricultured cell sheet captured with a fluorescence microscope. The cell sheet was immunostained for insulin (red) and GFP (green). Nuclei are stained blue. Scale bar: 50 μm.

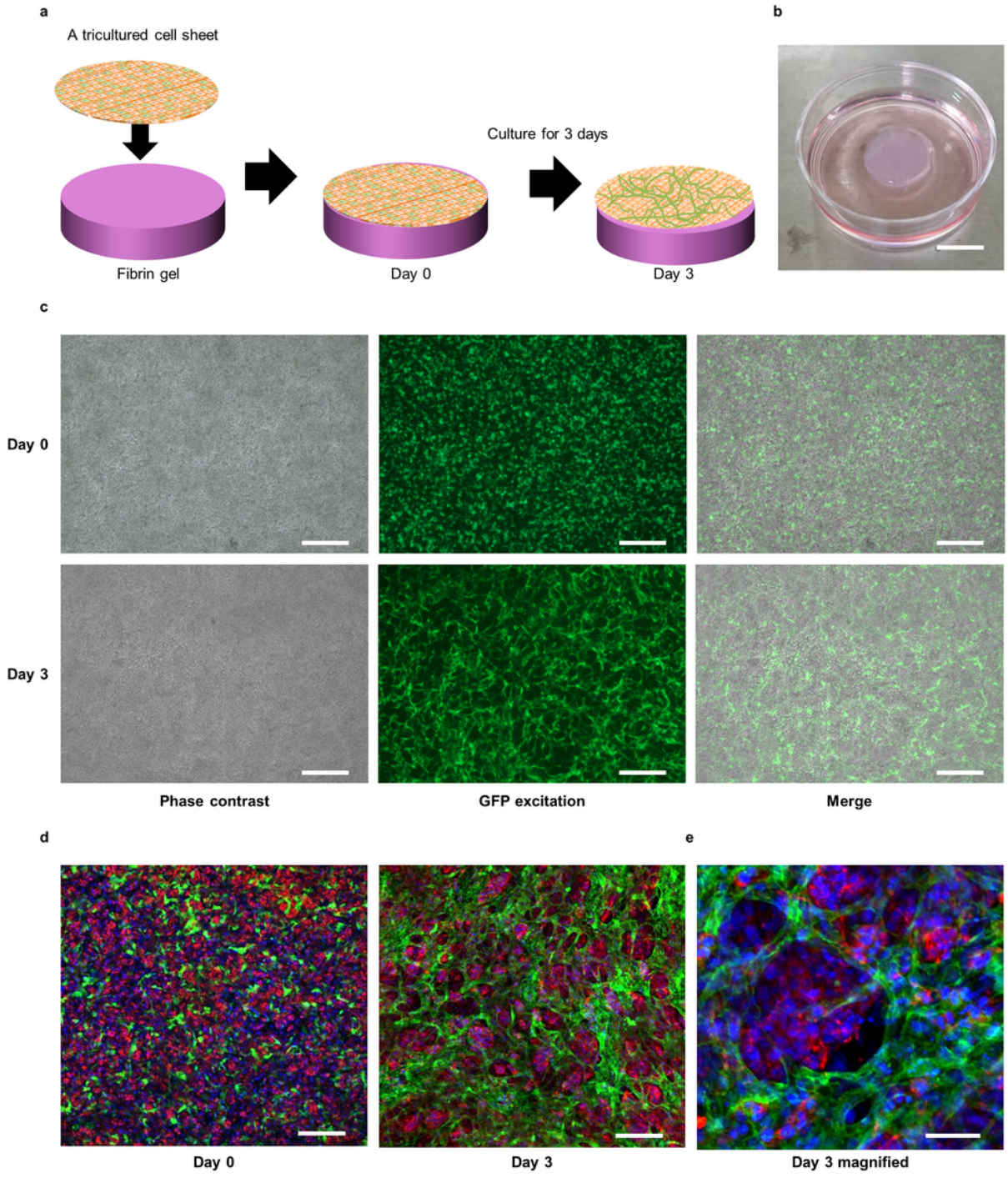

Figure 3

Changes in the morphology of a tricultured cell sheet after transplantation onto a fibrin gel

(a) Schematic summary of the experimental procedure. A tricultured cell sheet was harvested, transplanted onto a cylindrical fibrin gel and cultured in medium for 3 days. (b) Representative image of a tricultured cell sheet on a fibrin gel captured with a regular camera. Scale bar: 1 cm. (c) Representative images of a tricultured cell sheet captured with a phase-contrast microscope and a fluorescence stereomicroscope on days 0 and 3. Green indicates GFP-HUVECs. Scale bar: 500 μm. (d) Representative images of a tricultured cell sheet captured with a confocal fluorescence microscope on days 0 and 3. The cell sheet was immunostained for insulin (red) and GFP (green). Nuclei are stained blue. Scale bar: 200 μm. (e) Magnified image of (d) on day 3. Scale bar: 50 μm.

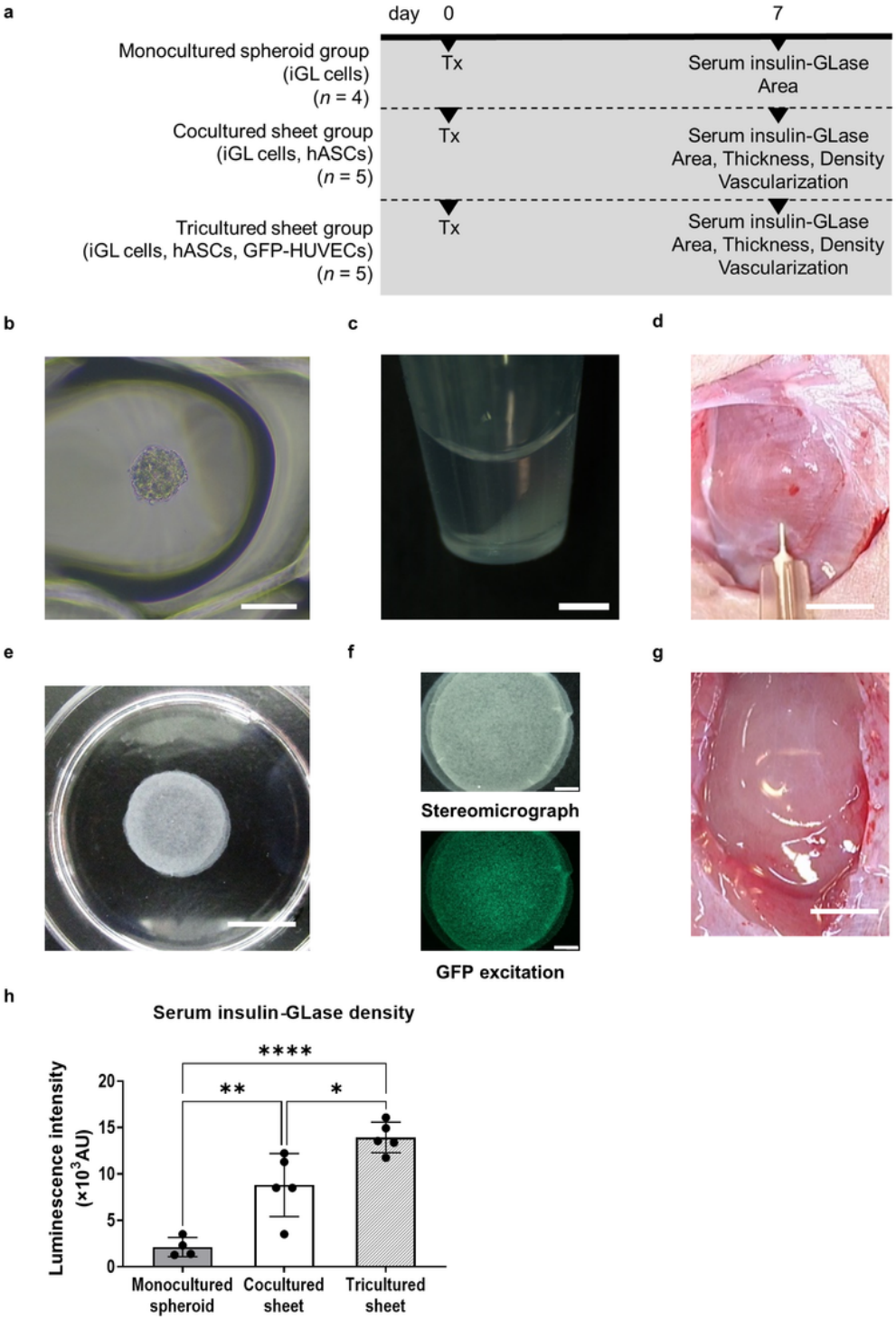

Figure 4

Transplantation of islet β-cells *in vivo* and insulin secretion by engrafted iGL cells

(a) Design of the animal experiments. The experimental groups, number of rats per group and indexes measured are shown. Area: measurement of the area of the engrafted islet β-cells; Density: measurement of the density of the islet β-cells in the engrafted sheets; Serum Insulin-GLase: bioluminescence

experiments to measure serum insulin-GLase; Thickness: measurement of the thickness of the engrafted sheets; Tx: cell transplantation (as sheets or spheroids); Vascularization: measurement of blood vessel density in the engrafted sheets. (b) Representative image of a spheroid in a microwell captured with a phase-contrast microscope. Scale bar: 100 μm. (c) Image of a suspension of spheroids in a microtube captured with a stereomicroscope. Scale bar: 2 mm. (d) Image acquired with a regular camera showing the transplantation of spheroids by injection into a muscle. Scale bar: 10 mm. (e) Representative image of a triple-layered tricultured cell sheet construct captured with a regular camera. The triple-layered construct was made by stacking three tricultured cell sheets. Scale bar: 10 mm. (f) Representative images of a triple-layered tricultured cell sheet construct captured with a stereomicroscope (upper) or fluorescence stereomicroscope (lower). Scale bar: 2 mm. (g) Image captured with a regular camera showing a triple-layered cell sheet construct being transplanted onto rat muscle. Scale bar: 10 mm. (h) Serum levels of insulin secreted by the engrafted iGL cells, evaluated from the luminescence intensity of insulin-GLase. The values are shown as the mean ± SDM (monocultured spheroid group, $n = 4$; other groups, $n = 5$). * $P < 0.05$, ** $P < 0.01$ and **** $P < 0.0001$.

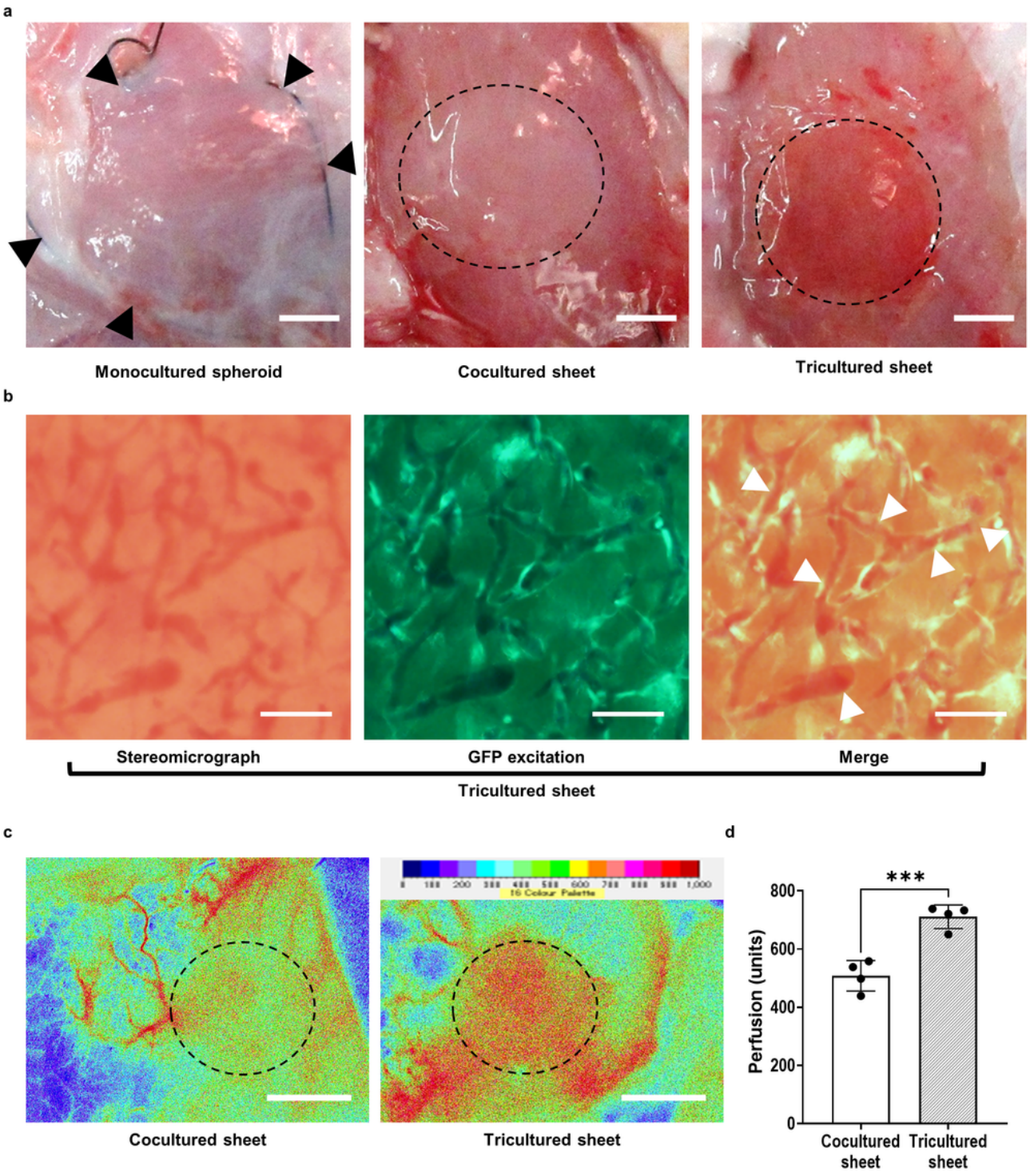

Figure 5

Morphology and blood perfusion of the transplanted region at 7 days after transplantation *in vivo*.

(a) Representative images captured by a regular camera showing the relevant region for each experimental condition at 7 days after transplantation. The region injected with monocultured spheroids is marked by a suture line (arrowheads, left). The dotted circles indicate engrafted cell sheets (middle and

right). Scale bar: 2 mm. (b) Representative images of a transplanted tricultured cell sheet captured by a stereomicroscope (left) and fluorescence stereomicroscope (middle). The merged images are shown on the right. The engrafted GFP-HUVECs formed tubular structures that contained the recipient rat's blood (white arrows). Scale bar: 100 μm. (c) Representative images of perfusion signals for a transplanted tricultured cell sheet and a transplanted cocultured cell sheet. The images were acquired using a laser Doppler perfusion system. Each dotted circle indicates the region of the engrafted cell sheet. Scale bar: 5 mm. (d) Comparison of the perfusion value between engrafted tricultured cell sheets and engrafted cocultured cell sheets. The values are shown as the mean ± SDM (n = 4 per group). *** $P < 0.001$.

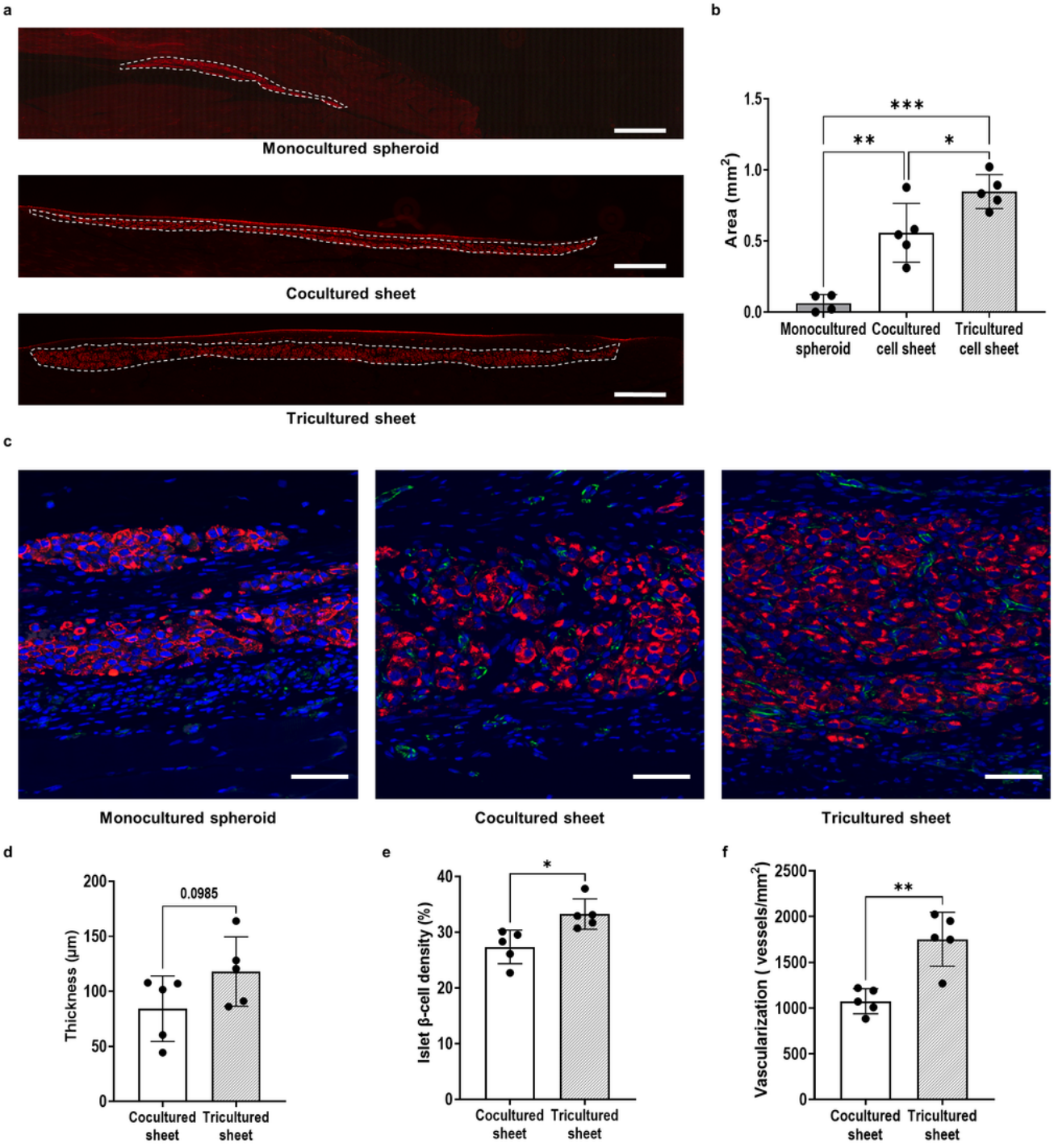

Figure 6

Histological evaluations of engrafted islet β-cells and blood vessels

(a) Representative immunofluorescence images for the three experimental groups showing the entire region in which islet β-cells had engrafted onto rat muscle. The islet β-cells were immunostained for insulin (red). The white dashed lines denote the engrafted islet β-cells. Scale bar: 1 mm. (b) Area of the

engrafted islet β-cells. The values are shown as the mean ± SDM (monocultured spheroid group, $n = 4$; other groups, $n = 5$). * $P < 0.05$, ** $P < 0.01$ and *** $P < 0.001$. (c) Representative immunofluorescence images obtained with a confocal microscope showing the region in which islet β-cells had engrafted. Islet β-cells were immunostained for insulin (red), and vascular endothelial cells were immunostained for CD31 (green). Scale bar: 50 μm. (d) Thickness of the engrafted cell sheets. (e) Islet β-cell density in the engrafted cell sheets. (f) Blood vessel density in the engrafted cell sheets. The values in (d–f) are shown as the mean ± SDM ($n = 5$ per group). * $P < 0.05$ and ** $P < 0.01$.

Supplementary Files

This is a list of supplementary files associated with this preprint. Click to download.

- supplementaryvideo1.avi
- supplementaryvideo2.avi
- supplementaryvideo3.avi
- supplementaryvideo4.mp4
- supplementaryvideo5.mp4
- 20220727finalSupplementaryInformationforsubmit.docx